Magnetic anisotropy and magnetic phase transitions in $R\mathrm{Fe}_{10}\mathrm{Mo}_2$ (R=Pr, Nd, Sm, Dy, Ho, Er, Tm)

K. Yu. Guslienko,* E. H. C. P. Sinnecker,† and R. Grossinger
Institute for Experimental Physics, Technical University of Vienna, Wiedner Hauptstrasse 8-10, A-1040 Vienna, Austria
(Received 29 August 1996)

$R\mathrm{Fe}_{10}\mathrm{Mo}_2$ (R=Pr, Sm, Nd, Dy, Ho, Er, Tm) intermetallics were investigated by studying the temperature- or field-induced spin-reorientation transitions (SRT's). The temperature dependence of the magnetic anisotropy field was determined by means of the singular point-detection technique for the polycrystalline samples of $\mathrm{YFe}_{10}\mathrm{Mo}_2$, $\mathrm{NdFe}_{10}\mathrm{Mo}_2$, $\mathrm{DyFe}_{10}\mathrm{Mo}_2$, and $\mathrm{ErFe}_{10}\mathrm{Mo}_2$. Main emphasis was given to the theoretical analysis of the magnetic anisotropy constants and the magnetic phase transitions. The temperature dependences of the rare-earth anisotropy constants were calculated using the single-ion model within linear theory. The applicability of the linear theory of the R anisotropy is discussed. It is shown that the accuracy of this theory increases considerably with increasing temperature. Fitting the experimental data, a set of the crystal field and exchange field parameters for the rare-earth R^{3+} ions was deduced. The observed SRT's and first-order magnetization processes (FOMP's) were explained and classified. FOMP-like transitions in $\mathrm{PrFe}_{10}\mathrm{Mo}_2$, $\mathrm{HoFe}_{10}\mathrm{Mo}_2$, and $\mathrm{ErFe}_{10}\mathrm{Mo}_2$ were identified. The temperature dependence of the FOMP fields was calculated for $\mathrm{HoFe}_{10}\mathrm{Mo}_2$ and $\mathrm{ErFe}_{10}\mathrm{Mo}_2$. The physical origin of a low-temperature anomaly in the magnetization process is discussed for $\mathrm{SmFe}_{10}\mathrm{Mo}_2$. The spin-reorientation transitions in $\mathrm{ErFe}_{10}\mathrm{Mo}_2$ and $\mathrm{TmFe}_{10}\mathrm{Mo}_2$ are determined to be of first order with a discontinuous jump of the magnetization. The SRT's detected in $\mathrm{NdFe}_{10}\mathrm{Mo}_2$ and $\mathrm{DyFe}_{10}\mathrm{Mo}_2$ are of second order. The calculated temperature dependences of the anisotropy fields for $\mathrm{DyFe}_{10}\mathrm{Mo}_2$ and $\mathrm{NdFe}_{10}\mathrm{Mo}_2$ are in good agreement with the experimental data over a wide temperature range. FOMP's are predicted at low temperatures for $\mathrm{NdFe}_{10}\mathrm{Mo}_2$, $\mathrm{DyFe}_{10}\mathrm{Mo}_2$, and $\mathrm{TmFe}_{10}\mathrm{Mo}_2$. [S0163-1829(96)04846-X]

I. INTRODUCTION

Intermetallic compounds, in which the magnetism of the rare-earth ions with localized magnetic $4f$ electrons is combined with that of the itinerant $3d$ transition metals, present an important class of magnetic materials. These materials are interesting for fundamental studies as well as from an applications point of view. Recently interest has been focused on the ternary intermetallics $R(\mathrm{Fe,M})_{12}$ (R=rare earth, M =Ti, Mo, V, . . .) due to their potential applications as permanent magnets and their various magnetic structures and magnetic phase transitions.

Magnetic anisotropy is one of the fundamental intrinsic properties of the magnetic materials and attracts ever-growing attention by both experimentalists and theoreticians. These compounds reveal a large magnetic anisotropy (mainly arising from the R sublattice) as well as large magnetization. The main function of the nonmagnetic M elements is to stabilize the ThMn_{12} structure. The rare-earth contribution to the resulting anisotropy of the $R(\mathrm{Fe},M)_{12}$ intermetallics is determined not only by the second-order crystal electric field (CEF) term but, in general, by the fourth- and sixth-order terms. It is known that, due to the high-order CEF terms, the easy magnetization direction (EMD) can deviate from the c axis. That is why many temperature- and magnetic-field-induced spin-reorientation transitions (SRT's) are observed in the $R(\mathrm{Fe},M)_{12}$, especially in the $R\mathrm{Fe}_{10}\mathrm{Mo}_2$ intermetallics. These compounds crystallize in the tetragonal ThMn_{12} structure with the space group $I4/mmm$. The contribution to the total magnetic anisotropy from the Fe sublattice favors the c axis. There is only one type of rare-earth crystallographic site and three crystallographically inequivalent Fe sites. With decreasing temperature the influence of the rare-earth anisotropy increases considerably which leads in the case of an opposite sign of the R anisotropy to temperature-induced SRT's. In $\mathrm{NdFe}_{10}\mathrm{Mo}_2$ a SRT occurs at T_s=147 K, in $\mathrm{DyFe}_{10}\mathrm{Mo}_2$ at 137 K, in $\mathrm{ErFe}_{10}\mathrm{Mo}_2$ at 180 K, whereas in $\mathrm{TmFe}_{10}\mathrm{Mo}_2$ at T_s=166 K.[1,2] First-order magnetization processes (FOMP's) or FOMP-like transitions were detected at 4.2 K in $R\mathrm{Fe}_{10}\mathrm{Mo}_2$ (R=Pr,Sm,Ho,Er).[1] It is proposed in Ref. 1 that the physical origin of a low-temperature anomaly found in the differential susceptibility dM/dH in $\mathrm{SmFe}_{10}\mathrm{Mo}_2$ is not due to a FOMP but caused by a continuous rotation of the magnetization.

The EMD in $\mathrm{PrFe}_{10}\mathrm{Mo}_2$ and $\mathrm{SmFe}_{10}\mathrm{Mo}_2$ lies in the basal plane or parallel to the c axis, respectively,[1] over the whole temperature range up to the Curie point. The situation in $\mathrm{NdFe}_{10}\mathrm{Mo}_2$ is more complex.

Measuring aligned samples of $\mathrm{NdFe}_{10}\mathrm{Mo}_2$ a SRT was observed in Refs. 1,2 and supposed to be a SRT from ''easy axis'' to ''easy cone.'' However an ''easy plane'' state was reported in Refs. 3 and 4 at room temperature. Two SRT's were detected in (Ref. 5): ''easy axis''–''easy cone'' above room temperature and ''easy cone''–''easy plane'' at 180 K. Wang *et al.*[6] found a SRT at T_s=155 in $\mathrm{NdFe}_{10}\mathrm{Mo}_2$. A conical magnetic moment configuration was proposed at a temperature below T_s.[6]

No indication of a SRT or a first-order magnetization process was found for $\mathrm{TbFe}_{10}\mathrm{Mo}_2$ according to Ref. 1. The SRT observed for $\mathrm{DyFe}_{10}\mathrm{Mo}_2$ is supposed to be from easy axis to easy cone[1] or from easy axis to easy plane due to Ref. 7. The nature of the SRT's in $\mathrm{DyFe}_{10}\mathrm{Mo}_2$ at T_s=130 K and in

$ErFe_{10}Mo_2$ at 120 K was not determined by Ref. 8. The SRT's observed in $ErFe_{10}Mo_2$ and $TmFe_{10}Mo_2$ by Ref. 1 were supposed to be SRT's from easy axis to easy cone. Direct evidence for this supposition is absent now. The absence of any singularities in d^2M/dt^2 versus H applying the singular point detection (SPD) technique for $ErFe_{10}Mo_2$ and $TmFe_{10}Mo_2$ can be taken as a hint that the magnetic anisotropy is either not axial or very low.[1,7]

Due to the complex behavior of the magnetic anisotropy, the type of SRT's and FOMP's in nearly all $RFe_{10}Mo_2$ is not clear up to now. From the slope of the magnetization curve breaking up the ferrimagnetic alignment in high fields, the values of the exchange field coefficients $n_{R\mathrm{Fe}}$ in $RFe_{10}Mo_2$ were recently found for the heavy rare-earth (R=Dy,Ho,Er,Tm) compounds.[1]

The crystal field and exchange field (for the light rare-earth ions) parameters are unknown. Direct measurements of the intersublattice exchange fields given in Ref. 1 deliver values for calculating the SRT and FOMP transitions. The anisotropy fields of the $RFe_{10}Mo_2$ (R=Nd,Dy,Er) intermetallics, in which the SRT's take place, and of $YFe_{10}Mo_2$ were measured over a wide temperature range using the SPD technique. In the present paper the experimentally observed temperature dependence of the anisotropy fields $H_A(T)$ as well as the first-order magnetization fields H_{cr} at 4.2 K,[1] and additionally the SRT temperatures,[1] are used in order to find the crystal and exchange field parameters for the $RFe_{10}Mo_2$ (R=Pr,Nd,Dy,Ho,Er,Tm) intermetallics within the single-ion rare-earth anisotropy model. The explanation and classification of the spin-reorientation transitions and first-order magnetization processes based on the found model parameters is the aim of the present paper. The experimental procedures are described in Sec. II. In Sec. III the details are given of the anisotropy and FOMP field calculations in the framework of the linear theory for a two-sublattice ferrimagnet. Analysis of the applicability of this theory based on the second-order corrections to the magnetic anisotropy constants is also given in Sec. III. An explanation of the magnetic anisotropy, SRT's and FOMP-like transitions in these compounds is given on the basis of the found model parameters in Sec. IV. A summary is presented in Sec. V.

II. EXPERIMENTAL DETAILS

The polycrystalline samples $RFe_{10}Mo_2$ with R=Y,Nd,Dy,Er were prepared by induction melting the stoichiometric amounts of the constituents under argon atmosphere. The starting materials of a purity of 99.99 wt% were used. The ingots were remelted four times in order to achieve homogeneity. The as-cast ingots were wrapped in Ta foil and sealed in a pre-evacuated and then argon-gas-filled quartz tube, followed by annealing at 1373 K for four weeks. The annealed samples were then water quenched and their phase content was checked by x-ray diffraction using Co $K\alpha$ radiation and by optical microscopy. All obtained samples showed a main phase with the tetragonal $ThMn_{12}$ structure. Traces of the elemental Fe were detected in all samples (below 5%). It is assumed that the soft magnetic impurity phases give no influence on the position of the SPD peak.

Magnetically aligned samples of a cylindrical shape were prepared by aligning fine powder particles (diameter is smaller than 40 μm) at room temperature applying a magnetic field of about 1 T perpendicular to the cylinder axis. Their directions were fixed with epoxy resin.

The temperature dependence of the magnetic anisotropy field $H_A(T)$ was determined by means of the SPD technique in a pulsed-field magnetometer which can be operated from 4.2 to 1000 K with a maximum field of 30 T. Polycrystalline samples of $YFe_{10}Mo_2$, $DyFe_{10}Mo_2$ and the aligned $NdFe_{10}Mo_2$, $ErFe_{10}Mo_2$ samples were used for the measurements.

III. METHOD OF CALCULATION

Magnetocrystalline anisotropy of the rare-earth (R) –transition metal (T) intermetallics is separated within the framework of a two-sublattice model into two parts, the R-sublattice anisotropy and the T-sublattice anisotropy. The R-anisotropy originates from the interaction between the aspherical electrostatic potential at the R site due to all other electrons in the lattice and the aspherical charge density of the unfilled $4f$ shell of the rare earths.

For calculating the temperature dependence of the rare-earth anisotropy constants the single-ion model was used because of the highly localized nature of the rare-earth $4f$ shell. The detailed description of this model was given in Ref. 9. A two-sublattice molecular field theory was used to describe the temperature dependences of the Fe- and R-sublattice magnetizations. This theory describes quite accurately the temperature dependence of the magnetization in the $RFe_{10}Mo_2$ intermetallics as shown in Ref. 10. The results[10] suggest that the magnetizations of the Fe and R sublattices are nearly collinear within a wide temperature range. For the tetragonal symmetry of the $ThMn_{12}$ structure only the crystal-field parameters A_{20}, A_{40}, A_{44}, A_{60}, A_{64} are necessary according to the symmetry of the crystal. The single-ion rare-earth Hamiltonian for a ground-state multiplet with an angular momentum J can be written as

$$H_R = H_{\mathrm{ex}} + H_{\mathrm{CF}} + H_Z, \tag{1}$$

where $H_{\mathrm{ex}} = 2(g_J - 1)\mu_B \mathbf{J}\cdot\mathbf{H}_{\mathrm{ex}}$ describes the isotropic exchange coupling energy with the iron sublattice, $H_{\mathrm{CF}} = \Sigma \theta_n A_{nm} C_m^n(\mathbf{J})$ is the crystal-field Hamiltonian decomposed by the irreducible tensor operators $C_m^n(\mathbf{J})$ which are proportional to the equivalent operators given by Ref. 11, θ_n are the Stevens factors and $H_Z = g_J \mu_B \mathbf{J}\cdot\mathbf{H}$ describes the Zeeman energy in an external magnetic field.

The total free energy consists of the Fe and R contributions and is given by

$$F = -k_B T \ln Z_R + K_{1\mathrm{Fe}} \sin^2\theta - \mathbf{M}_{\mathrm{Fe}}\cdot\mathbf{H},$$

$$Z_R = Sp(\exp(-\beta H_R)), \quad \beta = 1/(k_B T), \tag{2}$$

where $K_{1\mathrm{Fe}}$ and $\mathbf{M}_{\mathrm{Fe}}$ are the anisotropy constant and the magnetic moment of the Fe sublattice per formula unit, respectively. The values of $K_{1\mathrm{Fe}}$ and M_{Fe} are assumed to be the same as those found in $YFe_{10}Mo_2$ after scaling for the different Curie temperatures. To estimate $M_{\mathrm{Fe}}(T)$ a Brillouin-function approximation with $M_{\mathrm{Fe}}(0) = 14.06\mu_B$/f.u. (Ref. 1) was used. The values of $K_{1\mathrm{Fe}}(T)$ for $YFe_{10}Mo_2$ were calculated over a wide temperature region using the

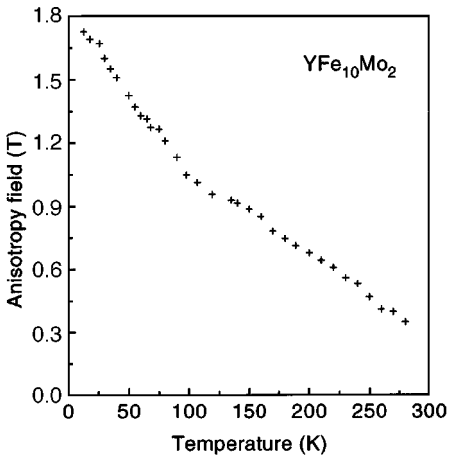

FIG. 1. Temperature dependence of the anisotropy field for $YFe_{10}Mo_2$.

formula $K_{1\mathrm{Fe}}(T)=K_{1\mathrm{Fe}}(0)(1-\alpha T/T_c)\sigma^3(T)$, where $\sigma(T)=M_{\mathrm{Fe}}(T)/M_{\mathrm{Fe}}(0)$. The coefficient $\alpha=0.625$ and $K_{1\mathrm{Fe}}(0)=7.60$ K/f.u. were found from a least-squares fitting procedure using the equation $K_1(T)=\mu_0 H_A(T)M_{\mathrm{Fe}}(T)/2$ giving the temperature dependence of $K_{1\mathrm{Fe}}(T)$. The anisotropy fields $H_A(T)$ for $YFe_{10}Mo_2$ were determined by the SPD technique within a temperature region 10–280 K (Fig. 1). A correction for the demagnetizing field was done. The Fe-ion magnetic moment $1.41\mu_B$ and the Fe-anisotropy constant $K_{1\mathrm{Fe}}$ (4.2 K)=7.60 K/f.u. are smaller than the ones for $YFe_{11}Ti$.[12]

The experimental data obtained by the SPD technique on the polycrystalline and magnetically aligned samples will be used in the present investigation. The contribution of the basal plane anisotropy constants K_2', K_3' are reduced to zero by averaging the azimuthal angle ϕ. Therefore the basal plane anisotropy (given by the A_{44}, A_{64} crystal-field parameters) does not contribute to the measured anisotropy field or critical field of the first-order magnetization process. The uniaxial contribution from the rare-earth sublattice to the magnetic anisotropy within the linear theory is given by

$$\langle H_{\mathrm{CF}}\rangle = K_{1R}(\xi)\sin^2\theta + K_{2R}(\xi)\sin^4\theta + K_{3R}(\xi)\sin^6\theta, \quad (3)$$

where $\xi=2(g_J-1)\mu_B JH/k_BT$. The rare-earth contributions according to the resulting anisotropy costants are

$$\begin{aligned} K_{1R}(\xi) &= -\tfrac{3}{2}\,\theta_2 J^2 A_{20} B_J^2(\xi) - 5\,\theta_4 J^4 A_{40} B_J^4(\xi) \\ &\quad - \tfrac{21}{2}\,\theta_6 J^6 A_{60} B_J^6(\xi), \\ K_{2R} &= \tfrac{35}{8}\,\theta_4 J^4 A_{40} B_J^4(\xi) + \tfrac{189}{8}\,\theta_6 J^6 A_{60} B_J^6(\xi), \\ K_{3R}(\xi) &= -\tfrac{231}{16}\,\theta_6 J^6 A_{60} B_J^6(\xi). \end{aligned} \quad (4)$$

In Eq. (4) the definition $\langle C_m^n(\mathbf{J}')\rangle = J^n B_J^n(\xi)$ was used, where $B_J^n(\xi)$ are the generalized Brillouin functions.[14] The temperature dependence of $H_{\mathrm{ex}}(T)$ is supposed to be proportional to $M_{\mathrm{Fe}}(T)$. The resulting anisotropy constants are $K_1=K_{1\mathrm{Fe}}+K_{1R}$, $K_2=K_{2R}$, $K_3=K_{3R}$. The definition of the anisotropy field applying an external magnetic field in the hard direction ($\theta=\pi/2$ for the easy axis phase) is as follows:

$$H_A = -\frac{1}{M_S}\frac{\partial^2 F_A}{\partial\theta^2}\bigg|_{\theta=\pi/2}, \quad F_A = \langle H_{\mathrm{CF}}\rangle + K_{1\mathrm{Fe}}\sin^2\theta. \quad (5)$$

The total anisotropy field is given due to Eq. (5) by $H_A=2(K_1+2K_2+3K_3)/M_S$, where M_S is the total magnetization. This equation is valid for $R\mathrm{Fe}_{10}\mathrm{Mo}_2$ (R =Sm,Nd,Dy) over the whole temperature range of $H_A(T)$ as determined by the SPD technique. The temperature dependence of H_A was calculated by fitting the experimental data over a wide temperature range.

For the light rare earths the total magnetization is $M_s=M_{\mathrm{Fe}}+M_R$ whereas for heavy rare earths $M_s=M_{\mathrm{Fe}}-M_R$. $M_R(T)=M_R(0)B_J(\xi)$ and $M_R(0)=g_J J$ is the free R^{3+} rare-earth ion value.

In order to calculate the temperature dependence of the rare-earth anisotropy constants Eq. (4) a first-order perturbation theory is used. This linear theory works well for small CEF energy if the conditions $|A_{nm}|\ll\mu_B JH_{\mathrm{ex}}$ are fulfilled. More details about the applicability of the linear theory of the magnetic anisotropy in the $3d$-$4f$ intermetallics were given in Ref. 13 for the case $T=0$. This question is actual for the $R\mathrm{Fe}_{10}\mathrm{Mo}_2$ series because the measured values of the intersublattice exchange field and the Curie temperatures are not large.[1] In order to estimate the accuracy of the linear theory we calculated the second-order correction at finite temperature. According to Ref. 15 the second-order perturbation theory is as follows:

$$\begin{aligned} F_R &= F_{R0} - \beta^{-1}(x_1 + x_2 - \tfrac{1}{2}x_1^2), \\ x_1 &= -\beta Z_{R0}^{-1}\sum_\nu \exp(-\beta E_\nu)\langle \nu J|H_{\mathrm{CF}}|J\nu\rangle, \\ x_2 &= Z_{R0}^{-1}\sum_{\mu\nu}\exp(-\beta E_\nu)|\langle \mu J|H_{\mathrm{CF}}|J\nu\rangle|^2 \\ &\quad \times \frac{\exp[\beta(E_\nu-E_\mu)]-1-\beta(E_\nu-E_\mu)}{(E_\nu-E_\mu)^2}, \end{aligned} \quad (6)$$

where $|J\nu\rangle$ and E_ν are the eigenfunctions and the eigenvalues of the unperturbated rare-earth Hamiltonian (H_{ex}), $F_{R0}=-\beta^{-1}\ln Z_{R0}$ is the unperturbated rare-earth free energy, $\mu,\nu=J, J-1,\ldots,-J$.

Let us suppose that the second-order CEF term (A_{20}) gives the leading contribution to the rare-earth anisotropy constants and to the anisotropy field. Thus we get the second-order correction to the anisotropy field in the form[13]

$$\begin{aligned} H_A(T) &= H_A^{\mathrm{linear}}(T)[1+\varepsilon(T)], \\ \varepsilon(T) &= [\delta K_1(T) + 2\,\delta K_2(T)]K_1^{-1}(T), \end{aligned} \quad (7)$$

where the relative error of the linear theory $\varepsilon(T)$ depends strongly on temperature. δK_1, δK_2 are the second-order corrections to the anisotropy constants. The second-order CEF correction to the rare-earth magnetization δM_R is small compared with the total magnetization M_s and is neglected here.

Calculating the matrix elements of H_{CF}, $\varepsilon(T)$ can be written as follows:

$$\varepsilon(T)=-\frac{3}{8}\frac{A_{20}}{T_{\rm ex}}f(t),\quad t=T/T_c,\quad T_{\rm ex}=2\mu_B H_{\rm ex}(0), \tag{8}$$

$$f(t)=\frac{T_{\rm ex}}{T_c}\frac{1}{J^2 Z_{R0}(y)B_J^2(Jy)}\frac{\theta_2}{t}\left(\frac{[1-\exp(-y)]}{y}S_1(y)-\frac{[1-\exp(-2y)]}{4y}S_2(y)-\frac{3}{2}Z_{R0}^{-1}(y)S_3(y)\right),$$

$$S_1(y)=\sum_{\nu}(2\nu-1)^2(J+\nu)(J-\nu+1)\exp(\nu y),$$

$$S_3(y)=\sum_{\mu\nu}(\mu^2-\nu^2)^2\exp[(\mu+\nu)y],$$

$$S_2(y)=\sum_{\nu}(J+\nu)(J+\nu-1)(J-\nu+1)(J-\nu+2)\exp(\nu y),$$

$$y=y(t)=\frac{T_{\rm ex}}{T_c}|g_J-1|\frac{\sigma(t)}{t}.$$

The second-order correction is determined by the ratio $A_{20}/T_{\rm ex}$ as well as the function $f(t)$ which depends strongly on the temperature and on J. When the temperature increases, the absolute value of the function $f(t)$ decreases (Fig. 2) and therefore the second-order correction to the anisotropy field calculated within the linear theory decreases rapidly. The values of $f(t)$ are much bigger for R=Pr,Tm than that for R=Nd,Sm,Dy,Ho,Er at low temperatures $t=T/T_c<0.1$ (Fig. 2). The sign of $f(t)$ coincides with the sign of $\theta_2(J)$. For instance, the ratio $\varepsilon(T\to T_c)/\varepsilon(T\to 0)$ is 0.06 for Sm^{3+} and 0.03 for Pr^{3+} (if we take $T_{\rm ex}/T_c=0.5$). One has to be careful applying the linear theory if the ratio $A_{20}/T_{\rm ex}$ is about a unit and the low-temperature experimental data (the FOMP fields, for instance) are used for the fitting procedure. Equations (7) and (8) generalize the results given by Ref. 13 for the case of a finite temperature. The crystal-field parameters found within the linear theory will be effective parameters if $H_{\rm CF}\ll H_{\rm ex}$ is not fulfilled and ε is not small compared with the unit. This situation is realized for $PrFe_{10}Mo_2$. As shown below, the linear theory cannot explain the magnetization curve of $SmFe_{10}Mo_2$ at low temperatures.

A field-induced FOMP occurs due to the existence of two relative minima of the free energy. Following Ref. 16 two types of FOMP's can be distinguished: transition to the saturated state (type 1) or to a not-saturated state (type 2). Usually the FOMP's are observed at low temperatures when K_2, K_3 are not negligible. In order to calculate the critical fields of a type-1 FOMP and the corresponding magnetization jumps (between inequivalent magnetization directions), the equations for an uniaxial ferromagnet as given in Ref. 16 were used. The analysis of the total free energy Eq. (2) and its derivatives with respect to the magnetization angle θ delivers an analytical solution for the critical magnetization in the axial and perpendicular magnetic fields (parallel and perpendicular to the alignment direction).[16]

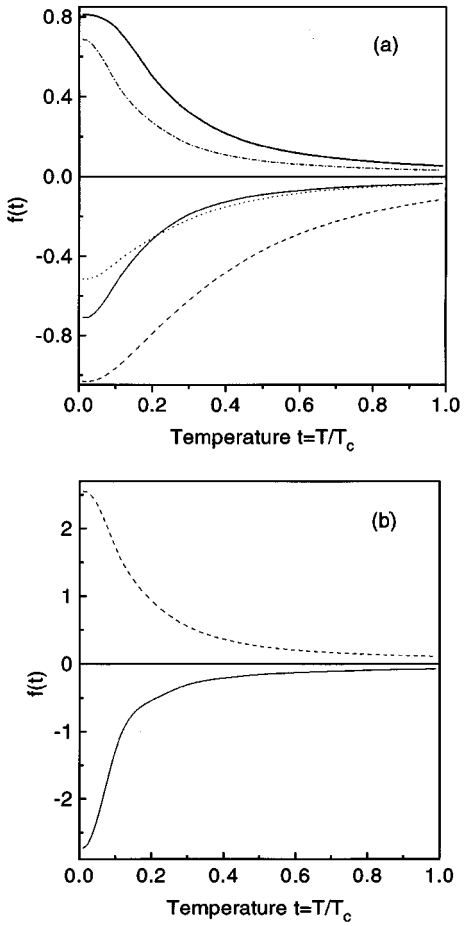

FIG. 2. Temperature dependence of the function $f(t)$ for the $R Fe_{10}Mo_2$ series (a) —— Nd, —— Sm, --- Dy, · · · · Ho, -·-·- Er; (b) —— Pr, --- Tm.

IV. RESULTS AND DISCUSSION

The experimental data for $R Fe_{10}Mo_2$ obtained in Ref. 1 and in the present paper are explained by the model described above. The temperature dependence of the rare-earth contribution to the total anisotropy energy is described analytically on the basis of the linear approximation. The measured anisotropy fields $H_A(T)$ for $YFe_{10}Mo_2$ were used to find the Fe-anisotropy constant. A_{40} and/or A_{60} crystal-field parameters for all rare-earth ions (except Sm) were scaled from $DyFe_{10}Mo_2$ by the relation $A_{n0}(R)=\langle r^n\rangle_R/\langle r^n\rangle_{\rm Dy}A_{n0}({\rm Dy})$. The values of $\langle r^n\rangle$ for the R ions were taken from Ref. 17. The crystal-field parameters calculated within this work are shown in Table I.

A. $PrFe_{10}Mo_2$ and $SmFe_{10}Mo_2$

The temperature dependences of the ac susceptibility and the magnetization reveal no anomalies up to the Curie temperature.[1] Applying Eqs. (2), (3), and (4) on the experimental data as obtained for $PrFe_{10}Mo_2$ (the FOMP field) allows to calculate a set of the crystal-field parameters: $A_{20}=-202$ K, $A_{40}=-76$ K, $A_{60}=70$ K (Table II). A type-2 FOMP (Ref. 16) takes place in $PrFe_{10}Mo_2$ at low temperatures. This FOMP was described by the equations given in Ref. 16. The experimental value of the FOMP field[1] at $T=4.2$ K was used for the fitting procedure. The anisotropy

TABLE I. Fitted crystal-field parameters for $R\mathrm{Fe}_{10}\mathrm{Mo}_2$. The units of $T_{ex}=2\mu_B H_{ex}(0)$, T_s and A_{nm} are in K. *A-C*, *A-P* are the easy axis–easy cone and easy axis–easy plane SRT's, respectively. *A*-1(2), *P*-1(2) denote the type 1(2) FOMP in the axial and perpendicular magnetic fields, respectively. T_s and T_{ex} (except $\mathrm{NdFe}_{10}\mathrm{Mo}_2$) are taken from Ref. 1.

	T_{ex}	A_{20}	A_{40}	A_{60}	T_s	SRT	FOMP	Remarks
$\mathrm{PrFe}_{10}\mathrm{Mo}_2$		−202	−76[a]	70[a]			*A*-2	
$\mathrm{NdFe}_{10}\mathrm{Mo}_2$	232	−95	−67[a]	57[a]	147	*A-C*		Low $H_A(T)$ Pred *A*-1
$\mathrm{DyFe}_{10}\mathrm{Mo}_2$	248	−2.3	−35	23	137	*A-C*		Pred *P*-1
$\mathrm{HoFe}_{10}\mathrm{Mo}_2$	194	10	−32[a]	21[a]			*P*-2	
$\mathrm{ErFe}_{10}\mathrm{Mo}_2$	149	139	−29[a]	19	180	*A-P*	*A*-2	Low $H_A(T)$
$\mathrm{TmFe}_{10}\mathrm{Mo}_2$	182	64	−27[a]	17[a]	166	*A-P*		Low $H_A(T)$

[a]Scaled from $\mathrm{DyFe}_{10}\mathrm{Mo}_2$.

constant K_2 is positive and K_1, K_3, $(K_1+2K_2+3K_3)$ are negative over the whole temperature range due to these crystal-field parameters and the signs of the Stevens factors θ_n for the Pr^{3+} ions. The easy plane phase is stable and therefore the SPD peaks in d^2M/dt^2 versus H are not observed over the whole temperature range. The calculated curve of $H_{cr}(T)$ using the fitted crystal-field parameters depends strongly on the intersublattice exchange field $T_{ex}=2\mu_B H_{ex}(0)$. Following Sec. III in $\mathrm{PrFe}_{10}\mathrm{Mo}_2$ due to a main contribution of A_{20} and the estimation $T_{ex}\simeq 300$ K, these parameters are the effective crystal-field parameters.

For $\mathrm{SmFe}_{10}\mathrm{Mo}_2$ no SRT was observed between 4.2 K and the Curie temperature. This means that $K_1(T)>0$ and an ''easy axis'' phase is stable. An anomalous increase of the magnetization at low temperatures was detected applying a magnetic field perpendicular to the alignment direction.[1] If only the ground-state multiplet with $J=5/2$ is taken into account, one obtains $K_3=0$ within the linear theory due to $\theta_6=0$. The magnetization curve versus a perpendicular field $(m=M/M_s)$ can be calculated by minimizing Eq. (2) with respect to θ:

$$m(H)=\alpha\,\sinh\left[\frac{1}{3}\sinh^{-1}\left(\frac{H}{H_0}\right)\right],\quad K_2>0,$$

$$m=\sin\theta,\quad H_0=\frac{2K_1}{3M_s}\alpha, \tag{9}$$

$$m(H)=-\alpha\cos\left[\frac{1}{3}\cos^{-1}\left(\frac{H}{H_0}\right)+\frac{2}{3}\pi\right],$$

$$K_2<0,\quad \alpha=\left(\frac{2K_1}{3|K_2|}\right)^{1/2}. \tag{9'}$$

Equations (9) and (9′) are valid in the case of $H<H_A=2(K_1+2K_2)/M_s$. No singularity in $\partial M/\partial H$ versus H is found for $K_2>0$. Equation (9′) has a singularity of $\partial m/\partial H$ for $H=H_0$. But this singularity has no physical meaning because $H_0>H_A$. There exist a possibility of a type-1 FOMP if $K_2<0$ and $-1/2<K_2/K_1<-1/6$.[16] The critical magnetization and the critical FOMP field can be written as follows:[16]

$$m_{cr}=\frac{1}{3}\left[\left(-3\frac{K_1}{K_2}-2\right)^{1/2}-1\right],\quad H_{cr}=2\frac{m_{cr}}{M_s}(K_1+2K_2m_{cr}^2). \tag{10}$$

This possibility is not realized because $H_{cr}>H_A$, which is in contradiction to the experiment[1] where $H_{cr}<H_A$ was observed at the same temperatures. Therefore the low-temperature anomaly of $M(H)$ cannot be explained within the linear theory and nonlinear corrections which lead, in particular, to $K_3\not\equiv 0$ are necessary for $\mathrm{SmFe}_{10}\mathrm{Mo}_2$.

B. $\mathrm{NdFe}_{10}\mathrm{Mo}_2$

Fitting the experimental data of $H_A(T)$ $\mathrm{NdFe}_{10}\mathrm{Mo}_2$ a set of the rare-earth ion parameters are deduced: $T_{ex}=232$ K, $A_{20}=-95$ K, $A_{40}=-67$ K, $A_{60}=57$ K (Table I). T_{ex} is much lower than that of $\mathrm{NdFe}_{11}\mathrm{Ti}$.[9] From our experimental data it is evident that the magnetic anisotropy field is small. The equation $K_1(T_s)=0$ and the experimental values of $H_A(T)$ were used for the fits. The calculated cone angle θ_c in $\mathrm{NdFe}_{10}\mathrm{Mo}_2$ changes continuously with decreasing temperature and the SRT at $T_s=147$ K (Ref. 1) is of the second order. The present set of the Nd^{3+} crystal-field parameters leads to the prediction of a type-1 FOMP in the axial magnetic fields at low temperatures. But the FOMP field is small (<0.4 T). This may be the reason why no FOMP was detected in Refs. 1,2. Substituting Fe by Co for $\mathrm{NdFe}_{10-x}\mathrm{Co}_x\mathrm{Mo}_2$ at $x\geqslant 5$, no spin reorientation was found.[5]

The phase equilibrium conditions and therefore the critical temperatures T_s, as obtained for the single crystals as well as for the magnetically aligned samples, depend strongly on the magnetic field applied in the different directions. This may be the reason why these critical temperatures (especially for $\mathrm{NdFe}_{10}\mathrm{Mo}_2$ and $\mathrm{DyFe}_{10}\mathrm{Mo}_2$) reported in various works are so different. With the fitted crystal-field parameters the anisotropy constant K_2 is positive at high temperatures and negative (due to a negative contribution of A_{60}) at low temperatures. K_3 is positive over the whole temperature range for $\mathrm{NdFe}_{10}\mathrm{Mo}_2$.The first anisotropy constant K_1 is positive above T_s and changes the sign at T_s with decreasing temperature due to the negative contributions of A_{20} and A_{40}. So, the SRT in $\mathrm{NdFe}_{10}\mathrm{Mo}_2$ at $T_s=147$ K occurs due to a competition of the Fe and Nd contributions to K_1. The calculated curves of $H_A(T)$ as well as the experimental $H_A(T)$ for $\mathrm{NdFe}_{10}\mathrm{Mo}_2$ using the fitted crystal and

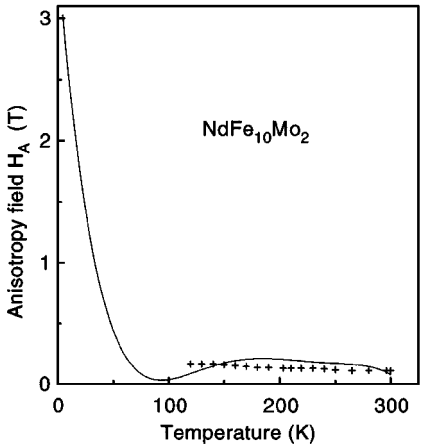

FIG. 3. Temperature dependence of the anisotropy field for $NdFe_{10}Mo_2$. The solid line represents the calculated, crosses (+) the experimental values.

exchange field parameters are shown in Fig. 3. The relative error of the linear theory is not large for all temperatures and has a negligible value above T_s (Table II). The reason of the small values of $H_A(T)$ measured above T_s is due to the calculated small values of the sum $K_1+2K_2+3K_3$ within 50–300 K. The small anisotropy of $NdFe_{10}Mo_2$ at room temperature leads to a poor alignment and, therefore, to a small difference between the magnetization curves measured parallel and perpendicular to the alignment direction.[1]

C. $DyFe_{10}Mo_2$

Fitting the experimental data of $H_A(T)$ for $DyFe_{10}Mo_2$ a set of the rare-earth ion parameters are deduced: $A_{20}=-2.3$ K, $A_{40}=-35$ K, $A_{60}=23$ K. The equation $K_1(T_s)=0$ and $T_{ex}=248$ K which was calculated after measurements[1] and the experimental values of the anisotropy field were used for the fitting procedure. The calculated cone angle θ_c in $DyFe_{10}Mo_2$ changes continuously with decreasing temperature and the SRT observed at $T_s=137$ K (Ref. 1) is of the second order. The present set of the Dy^{3+} crystal-field parameters leads to the prediction of a type-1 FOMP in a perpendicular magnetic field at low temperatures. With the fitted crystal-field parameters the anisotropy constant K_2 is positive and K_3 is negative over the whole temperature range in $DyFe_{10}Mo_2$ as was also calculated for $DyFe_{11}Ti$.[9] The first anisotropy constant K_1 is positive above $T_s=137$ K and changes the sign at T_s with decreasing temperature due to the negative contributions of A_{20}, A_{40}, and A_{60}. So, the SRT in $DyFe_{10}Mo_2$ occurs due to a competition of the Fe and Dy contributions to K_1. Due to the positive values of the sum $K_1+2K_2+3K_3$ which holds over the whole temperature region, a second SRT at low temperatures as proposed in $DyFe_{11}Ti$,[9] is not expected for $DyFe_{10}Mo_2$. The calculated values of $H_A(T)$ and $H_{cr}(T)$ as well as the experimental $H_A(T)$ for $DyFe_{10}Mo_2$ are shown in Figs. 4(a) and 4(b). The relative error of the linear theory $\varepsilon(T)$ is negligible over the whole temperature range (Table II).

TABLE II. The relative error of the linear theory of the R anisotropy for the $RFe_{10}Mo_2$ series. T_c (K) are taken from Ref. 1.

	T_c	$\varepsilon(T=4.2$ K)	$\varepsilon(T_s)\ 10^2$	Remarks
$NdFe_{10}Mo_2$	366	−0.109	−1.90	High-temp. fitting
$DyFe_{10}Mo_2$	335	−0.003	−0.16	High-temp. fitting
$HoFe_{10}Mo_2$	310	0.010	0.09[a]	
$ErFe_{10}Mo_2$	285	−0.240	−1.96	
$TmFe_{10}Mo_2$	258	−0.336	−2.49	High-temp. fitting

[a] $-\varepsilon(0.9T_c)$ for $HoFe_{10}Mo_2$.

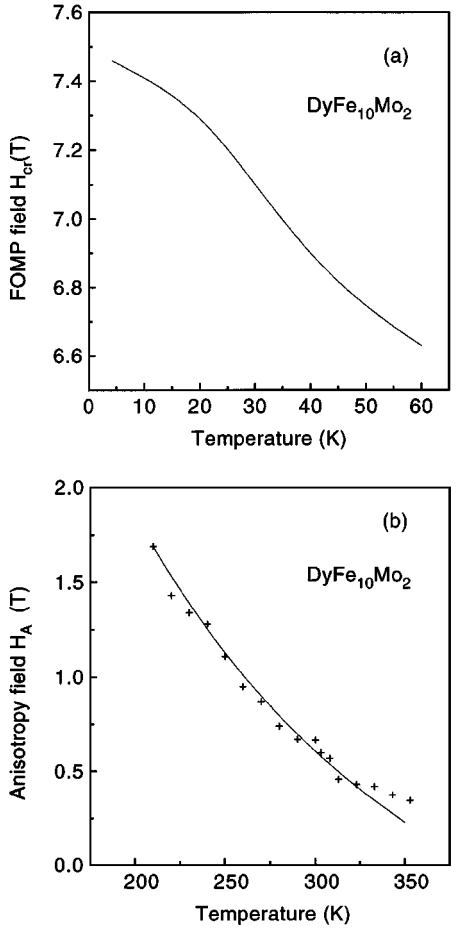

FIG. 4. Temperature dependence of the FOMP field (a) and the anisotropy field (b) for $DyFe_{10}Mo_2$. The solid lines represent the calculated, crosses (+) the experimental values.

D. $HoFe_{10}Mo_2$

The temperature dependence of the ac susceptibility and the magnetization give no evidence of the anomalies up to the Curie temperature.[1] A set of the crystal-field parameters $A_{20}=10$ K, $A_{40}=-32$ K, $A_{60}=21$ K (Table I) was obtained by applying Eqs. (2), (3), and (4) to the experimental data. In $HoFe_{10}Mo_2$ at low temperatures a type-2 FOMP in a perpendicular magnetic field is predicted. The calculated temperature dependences of the FOMP field and anisotropy field are shown in Fig. 5. The anisotropy field has a considerable high value at low temperatures. The experimental value of the FOMP field[1] at $T=4.2$ K and $T_{ex}=194$ K calculated from

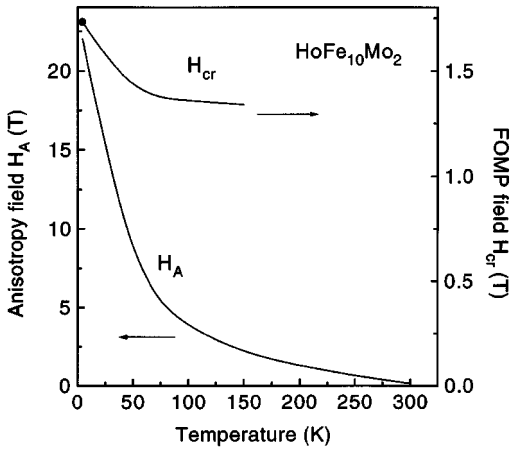

FIG. 5. Temperature dependence of the anisotropy field and the FOMP field for $HoFe_{10}Mo_2$. The solid lines represent the calculated, circle ($\otimes$) the experimental value (Ref. 1).

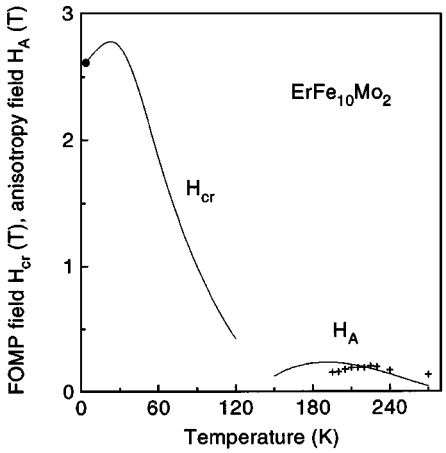

FIG. 6. Temperature dependence of the FOMP field and the anisotropy field for $ErFe_{10}Mo_2$. The solid lines represent the calculated, crosses (+) the experimental values. Circle ($\otimes$) represents the experimental value of the FOMP field (Ref. 1).

the measurements[1] were used for the fitting procedure. The values of $H_{cr}(T)$ are much lower than $H_A(T)$ at low temperatures which confirms the type-2 FOMP. The anisotropy constants K_1, K_3 are positive over the whole temperature range. A_{20}, A_{60} give positive and A_{40} gives a negative contribution to K_1. The calculated anisotropy constant K_2 is positive at high and negative (due to a negative contribution of A_{60}) at low temperatures (below 75 K). The $\varepsilon(T)$ is negligible for $HoFe_{10}Mo_2$ over the whole temperature range (Table II).

E. $ErFe_{10}Mo_2$

Two different possibilities exist to describe a SRT in $ErFe_{10}Mo_2$: (1) a SRT occurs due to a change in the sign of K_1 at T_s and $K_1(T_s)=0$; (2) a SRT occurs with $K_1>0$. By fitting experimental data as obtained for $ErFe_{10}Mo_2$ a set of the crystal-field parameters $A_{20}=139$ K, $A_{40}=-29$ K, $A_{60}=19$ K was calculated. $T_{ex}=149$ K was obtained from measurements.[1] A first-order SRT, easy axis–easy plane, at $T_s=180$ K with the condition $K_1(T_s)=0$ can be explained by the set of the crystal-field and exchange field parameters given above. However, that disagrees with the supposed SRT, easy axis–easy cone, in Ref. 1. A conical phase which can lead to a FOMP in a perpendicular field is not predicted over all temperatures. According to the calculations, the SRT temperature due to a first-order transition depends strongly on the external magnetic field. This fact is supported by the measurements[8] using aligned samples where $T_s=120$ K was detected.

According to Ref. 16 a type-2 first-order magnetization process in an axial magnetic field is predicted in $ErFe_{10}Mo_2$ at low temperatures. The calculated temperature dependence of the FOMP field is shown in Fig. 6. The experimental value of the FOMP field[1] at $T=4.2$ K was used during the fitting procedure. The anisotropy constant K_2 is calculated to be negative at high temperatures and positive (due to a positive contribution of A_{60}) at low temperatures. K_3 is negative over the whole temperature range. The parameters A_{20}, A_{60} give negative contributions to K_1. The contribution of the fourth and sixth crystal-field terms is negligible at T_s due to the small values of $\xi(T_s)$ and therefore the small values of the generalized Brillouin functions $B_J^{4,6}(\xi(T_s))$ which decrease rapidly with decreasing ξ.[14] For $ErFe_{10}Mo_2$ the parameter $\xi(T_s)\sim T_{ex}/T_s$ is much smaller than that for $ErFe_{11}Ti$.[9] The possibility $K_1(T_s)=0$ can be realized within the linear theory due to a large positive A_{20} value. The accuracy of the linear theory at $T=0$ estimated by A_{20} and T_{ex} is $\varepsilon(0)=-0.24$. Therefore the crystal-field parameters found for $EeFe_{10}Mo_2$ have the meaning of an effective CEF parameters and do not reproduce the scheme of the Er^{3+} energy levels correctly. The calculated and experimental values of $H_A(T)$ and $H_{cr}(T)$ of $ErFe_{10}Mo_2$ are shown in Fig. 6. The agreement of $H_A(T)$ is satisfactory since the experimental data were not used for the fits.

F. $TmFe_{10}Mo_2$

Similar to $ErFe_{10}Mo_2$, two different possibilities exist to describe a SRT in $TmFe_{10}Mo_2$. A set of the crystal-field parameters $A_{20}=64$ K, $A_{40}=-27$ K, $A_{60}=17$ K of $TmFe_{10}Mo_2$ was obtained by fitting experimental data.[1] The existence of a first order SRT, easy axis–easy plane, at $T_s=166$ K with the condition $K_1(T_s)=0$ can be explained by the set of the crystal-field and exchange field parameters given above. However, that is again in disagreement with the explanation proposed in Ref. 1 where an easy axis–easy cone transition was assumed. A conical phase is not stable within all temperatures. The anisotropy constant K_2 is calculated to be negative and K_3 positive over the whole temperature range. The parameters A_{40}, A_{60} give positive contributions to $K_1(T)$ and the SRT occurs due to a negative contribution of A_{20} to $K_1(T)$. The calculated values of $H_A(T)$ for $TmFe_{10}Mo_2$ are very low (<0.21 T). The estimated error of the linear theory at 4.2 K has considerable value (Table II). But low-temperature experimental data were not used for the fitting procedure and the CEF parameters are calculated with small error. The present set of the Tm^{3+} crystal-field parameters leads to the prediction of a type-1 FOMP in an axial magnetic field at low temperatures. This prediction based on the linear theory is only qualitative due to the estimated $\varepsilon(4.2\text{ K})=-0.34$.

The temperature dependences of the anisotropy fields in $R\mathrm{Fe}_{10}\mathrm{Mo}_2$ (R=Er,Tm) are the same (after scaling for the different Curie temperatures). The values of H_A are low due to the existence of a first-order SRT in these intermetallics. Based on the present calculations, the SRT's detected in $\mathrm{ErFe}_{10}\mathrm{Mo}_2$ and $\mathrm{TmFe}_{10}\mathrm{Mo}_2$ occur due to $K_1(T)=0$ at T_s. A_{20} is the leading parameter in determining the SRT's in $\mathrm{ErFe}_{10}\mathrm{Mo}_2$ and $\mathrm{TmFe}_{10}\mathrm{Mo}_2$ near the transition temperatures T_s.

V. SUMMARY

The investigation of the basic interactions (intersublattice exchange, anisotropy) of the rare-earth compounds $R\mathrm{Fe}_{10}\mathrm{Mo}_2$ (R=Pr,Nd,Dy,Ho,Er,Tm) was carried on by the complete analysis of its critical behavior versus applied magnetic field and temperature. In order to calculate the rare-earth anisotropy constants the linear modification of the general phenomenological crystal-field model was used. The single-ion model parameters were calculated for $R\mathrm{Fe}_{10}\mathrm{Mo}_2$ series on the basis of detailed analysis of the experimental data.

The spin-reorientation transitions and first-order magnetization processes observed in these intermetallics were explained and classified due to our calculations within the linear theory of the R anisotropy. The validity of this theory was tested for different rare-earth ions R calculating the temperature dependence of the second-order corrections. Type-1 first-order magnetization processes were predicted for R=Nd,Dy,Tm, that may be checked by direct measurements of the corresponding single crystals or polycrystalline aligned samples.

The field-induced transition detected at 4.2 K in $\mathrm{PrFe}_{10}\mathrm{Mo}_2$ applying a magnetic field parallel to the alignment direction is explained as a type-2 FOMP. The anomaly observed between 4 and 180 K in $\mathrm{SmFe}_{10}\mathrm{Mo}_2$ cannot be explained within the linear theory either as a first-order magnetization process or continuous rotation of the magnetization.

The spin-reorientation transition in $\mathrm{NdFe}_{10}\mathrm{Mo}_2$ and $\mathrm{DyFe}_{10}\mathrm{Mo}_2$ detected at T_s=147 K and 137 K in Ref. 1 is due to our calculations of the second order. The angle between M_s and the c axis increases continuously with decreasing temperature below T_s. A type-1 first-order magnetization process at low temperatures is predicted for $\mathrm{NdFe}_{10}\mathrm{Mo}_2$ applying a magnetic field parallel to the alignment direction and for $\mathrm{DyFe}_{10}\mathrm{Mo}_2$ applying a magnetic field perpendicular to the alignment direction. The SRT's and FOMP's in $\mathrm{NdFe}_{10}\mathrm{Mo}_2$ and $\mathrm{DyFe}_{10}\mathrm{Mo}_2$ are the consequence of the dominant contributions of the high-order CEF terms to the rare-earth anisotropy.

A transition detected at 4.2 K in $\mathrm{HoFe}_{10}\mathrm{Mo}_2$ when a magnetic field is applied perpendicular to the alignment direction is explained as a type-2 first-order magnetization process. High anisotropy fields are calculated for $\mathrm{HoFe}_{10}\mathrm{Mo}_2$ at low temperatures.

The first-order SRT's, easy axis–easy plane, are calculated with decreasing temperature in $\mathrm{ErFe}_{10}\mathrm{Mo}_2$ and $\mathrm{TmFe}_{10}\mathrm{Mo}_2$. In order to check this, e.g., specific heat has to be measured near T_s. A transition detected at 4.2 K in $\mathrm{ErFe}_{10}\mathrm{Mo}_2$ with a magnetic field applied parallel to the alignment direction is explained as a type-2 FOMP. A type-1 FOMP at low temperatures is predicted for $\mathrm{TmFe}_{10}\mathrm{Mo}_2$ when a magnetic field is applied parallel to the alignment direction. These SRT's are determined predominantly by the second-order CEF terms. Whereas the first-order magnetization processes are determined by the fourth- and sixth-order CEF terms.

The applicability of the linear theory of the rare-earth anisotropy depends strongly on temperature and the R-ion angular momentum J. The accuracy of this theory increases considerably with increasing temperature. In the $R\mathrm{Fe}_{10}\mathrm{Mo}_2$ series the linear theory works well for R=Nd,Dy,Ho over all temperature range and for R=Er,Tm at high temperatures (above T_s). The crystal-field parameter found for $\mathrm{PrFe}_{10}\mathrm{Mo}_2$ and $\mathrm{ErFe}_{10}\mathrm{Mo}_2$ within the linear theory have the meaning of an effective CEF parameter due to considerable error of this theory at low temperatures and use of the low-temperature experimental data for the fitting procedure.

The calculated curves of the magnetic anisotropy fields $H_A(T)$ for $R\mathrm{Fe}_{10}\mathrm{Mo}_2$ (R=Nd,Dy) are in good agreement with the experimental curves over a wide temperature range. The temperature dependences of the first-order magnetization process critical fields $H_{\mathrm{cr}}(T)$ are calculated for $R\mathrm{Fe}_{10}\mathrm{Mo}_2$ (R=Dy,Ho,Er).

ACKNOWLEDGMENTS

The authors are grateful to Dr. X. C. Kou for many discussions on the manuscript. This work was supported by the ''Fond zur Forderung der Wissenschaftlichen Forschung von Österreich'' under Grant Nos. S5604, S5605. K.Yu.G. thanks the ''Fond zur Forderung der Wissenschaftlichen Forschung'' of Austria for financial support by the Lise-Meitner Stipendium under Project No. M00175-PHY. E.H.C.P.S. thanks the OAD for financial support too.

*Permanent address: Inst. Magnetism, Vernadskogo 36, Kiev-142, Ukraine.

†Permanent address: Inst. de Fisica ''Gleb Wataghin,'' Universidade Estadual de Campinas 13083-970, Campinas, S.P., Brazil.

[1] X. C. Kou, R. Grossinger, G. Wiesinger, J. P. Liu, F. R. de Boer, I. Kleinschroth, and H. Kronmuller, Phys. Rev. B **51**, 8254 (1995).

[2] E. H. C. P. Sinnecker *et al.* (unpublished).

[3] A. S. Ermolenko, Y. V. Shcherbakova, G. V. Ivanova, and Y. V. Belozerov, Phys. Met. Metall. **70**, 52 (1990).

[4] Y. Z. Wang *et al.*, J. Appl. Phys. **73**, 6251 (1993).

[5] Xie Xu and S. A. Shaheen, J. Appl. Phys. **73**, 6248 (1993).

[6] Y. Z. Wang *et al.*, J. Appl. Phys. **75**, 6226 (1994).

[7] C. Christides, A. Kostikas, X. C. Kou, R. Grossinger, and D. Niarchos, J. Phys. C **5**, 8611 (1993).

[8] R. Tucker, Xie Xu, and S. A. Shaheeen, J. Appl. Phys. **75**, 6229 (1994).

[9] K. Yu. Guslienko, X. C. Kou, and R. Grossinger, J. Magn. Magn. Mater. **150**, 383 (1995).

[10] Xie Xu and S. A. Shaheen, J. Appl. Phys. **76**, 6754 (1994).

[11] K. W. H. Stevens, Proc. Phys. Soc. London Ser. A **65**, 209 (1952).
[12] Bo-Ping Hu, Hong-Shuo Li, J. M. D. Coey, and J. P. Gavigan, Phys. Rev. B **41**, 2221 (1990).
[13] M. D. Kuz'min and J. M. D. Coey, Phys. Rev. B **50**, 12 533 (1994).
[14] M. D. Kuz'min, Phys. Rev. B **46**, 8219 (1992).
[15] S. V. Tyablikov, *Methods of Quantum Theory of Magnetism* (Nauka, Moscow, 1965).
[16] G. Asti and F. Bolzoni, J. Magn. Magn. Mater. **20**, 29 (1980).
[17] A. J. Freeman and J. P. Desclaux, J. Magn. Magn. Mater. **12**, 11 (1979).